Quadrupole Induced Resonant Particle Transport in a Pure Electron Plasma

E. Gilson[1] and J. Fajans[2]

Department of Physics
University of California, Berkeley
Berkeley, California, 94720-7300

Abstract. We have performed experiments that explore the effects of a magnetic quadrupole field on a pure electron plasma confined in a Malmberg-Penning trap. We have developed a model which describes the shape of the plasma and shows that a certain class of resonant electrons follows trajectories that take them out of the plasma. Even though the quadrupole field destroys the cylindrical symmetry of the system, the theory predicts that if the electrons are off resonance, the lifetime of the plasma is not greatly affected by the quadrupole field, but near resonance the lifetime diminishes sharply. Preliminary experimental results show that the shape of the plasma and the plasma lifetime agree with the model. We are investigating the lifetime scaling with various experimental parameters such as the plasma length, density, and strength of the quadrupole field. This resonant particle transport may be detrimental to experiments which plan to use magnetic quadrupole neutral atom traps to confine anti-hydrogen created in double-well positron/anti-proton Malmberg-Penning traps.[3]

Resonant particle transport has long been suspected as the primary cause of plasma loss in Malmberg-Penning traps, but there is no conclusive experimental evidence to support this claim [1–5]. We have found experimental evidence for resonant particle transport when we apply a quadrupole magnetic field to our system. We have also measured the equilibrium shape of plasmas when a magnetic quadrupole perturbation is present. The results of this research apply directly to anti-hydrogen creation experiments proposed by the ATHENA and ATRAP collaborations. Malmberg-Penning traps will be used to confine positrons and anti-protons, which should recombine into anti-hydrogen. Quadrupole fields will be used to confine the neutral anti-hydrogen.

With an axially invariant transverse magnetic quadrupole field, the total magnetic field becomes

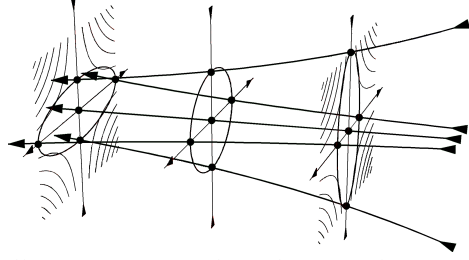$$\vec{B} = B_o\hat{z} + \beta_q(x\hat{x} - y\hat{y}), \tag{1}$$

[1] epgilson@physics.berkeley.edu
[2] joel@physics.berkeley.edu
[3] ATHENA and ATRAP Collaborations.

where $B_o\hat{z}$ is the standard axial field. The self electric fields of the plasma cause it

FIGURE 1. Adding a small transverse quadrupole perturbation to a constant axial field produces the field lines shown in this figure.

to $\vec{E} \times \vec{B}$ drift around the trap axis. When this rotation is slow compared to the time it takes an electron to bounce back and forth across the length of the plasma, the electrons follow the magnetic field lines shown in Fig. 1. The plasma has a circular cross section in the middle and has elliptical cross sections at both ends. The ellipses are rotated 90° from one another. When the rotation is fast compared to the bounce time, the plasma smears out into a cylinder.
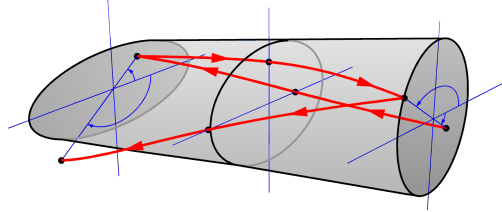
FIGURE 2. The equilibrium shape of a slowly rotating plasma. The lines with arrows (to be discussed later) show the trajectory followed by an outward moving resonant electron.

We measure the ellipticity ϵ and orientation θ of the plasma either by imaging the plasma or by measuring the image charge induced on the trap walls. When the plasma is rotating slowly, the quadrupole moment, as expected, is zero in the center of the plasma, has equal and opposite values at the ends of the plasma, and is proportional to β_q. When we image quickly and slowly rotating plasmas, we see the expected circular and elliptical shapes.

Theoretically, $\epsilon - 1$ should scale with β_q/B_o, and is in rough agreement with the data shown in Fig. 5. We do not understand the step in the data at $B_o \sim 400$ G. The variation in angle is reminiscent of the drive/response phase shift of a damped driven simple harmonic oscillator as it passes through resonance.

If the rotation rate is such that an electron makes a quarter revolution each time it travels the length of the plasma, the electron can move ever outwards or inwards (see the lines with arrows in Fig. 2). For a constant density plasma, the resonance condition is,

$$B_o = \frac{neL}{\pi\epsilon_o v_z}. \tag{2}$$

Resonant and near-resonant electrons traveling outwards can leave the plasma very quickly. Diffusion due to this mechanism can be large. There are higher order
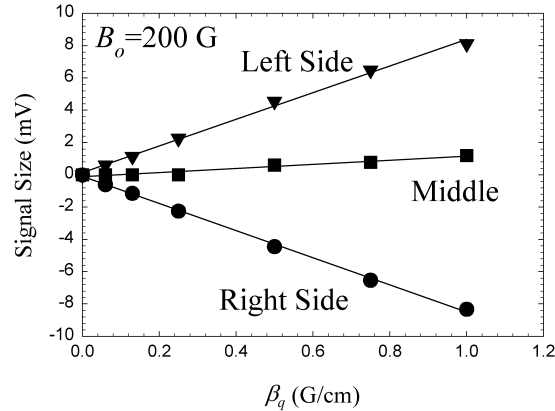
FIGURE 3. Measurements of quadrupole moment along the plasma's length show the axial dependence and β_q proportionality that we expect.
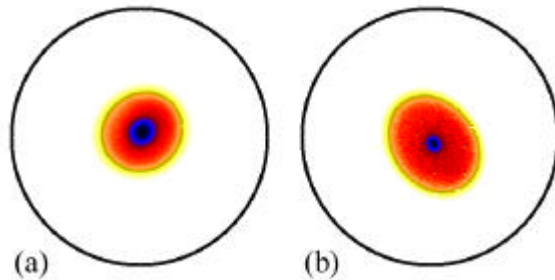
FIGURE 4. $\beta_q/B_o = 0.004$ cm^{-1}. (a) $B_o = 32.43$ G so the plasma is rotating quickly. We measure $\epsilon = 1.09$ and $\theta = 53.5°$. (b) $B_o = 500$ G so the plasma is rotating slowly. We measure $\epsilon = 1.26$ and $\theta = -37.5°$.

resonances in which the electron makes $N/4$ (N odd) revolutions as it travels across the plasma, but these are less important.

Above resonance, when the plasma is rotating slowly, the resonant velocity lies well within the electron distribution function $f(v)$. There are many resonant electrons and the quadrupole field has a strong effect. Well below resonance, when the plasma is rotating quickly, the resonant velocity falls in the tail of $f(v)$. Consequently, there are few resonant electrons and the quadrupole field has little effect.

This resonance effect can be seen in Fig. 6. Below resonance [Fig. 6 (a)], the application of the quadrupole field has no effect on the evolution of the central density as a function of time until the plasma expands enough so that the resonance condition is met. The plasma in Fig. 6 (b) begins above resonance so the quadrupole field has an immediate effect on the central density.

From a series of images taken at successive times, we measure the diffusion coefficient, D. The plasma images measure the z-averaged radial density profile $n(r,t)$, from which we compute $N(r,t) = \int_0^r n(r',t)2\pi r'\, dr'$.

We write the diffusion equation in polar coordinates, integrate once with respect to r and rearrange to yield

$$D(R) = \left. \frac{\partial N/\partial t}{2\pi R\, \partial n/\partial r}\right|_{r=R}. \tag{3}$$
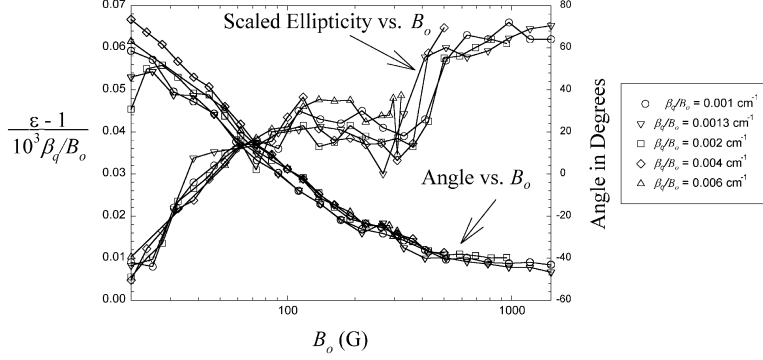
FIGURE 5. The scaled ellipticity and angle of the plasma as functions of B_o as measured from images such as those shown in Fig. 4.
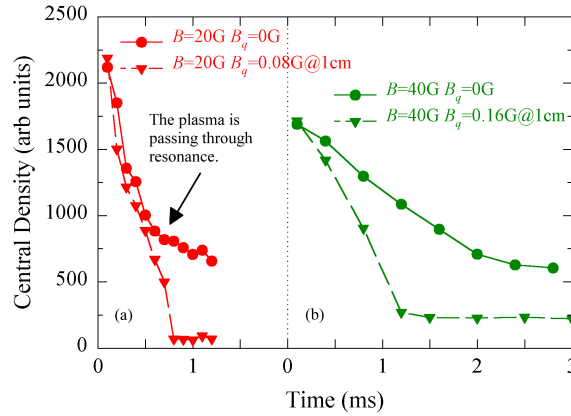

FIGURE 6. By comparing the time evolution of the central density with the quadrupole field on and off, we can separate the effects of the quadrupole field from other plasma loss mechanisms.

All θ variations have been neglected because the quadrupole field used in the diffusion experiments is typically small.

In Fig. 7 (a,b), we keep β_q/B_o fixed, as would be the case if the quadrupole field were due to imperfections in the main magnet coils. When $\beta_q \neq 0$, D is the sum of the diffusion due to both the quadrupole field and background processes. Below resonance, the quadrupole field has little effect, but above resonance it enhances diffusion. In Fig. 7 (c,d), we hold β_q fixed. For large B_o, the diffusion due to the quadrupole field becomes small and background processes dominate the diffusion. The anomalous structure in the background ($D_{\beta_q=0}$) data needs to be understood before further study can be completed.

By measuring the relative lifetimes using three different plasma lengths, we see that the location of the resonance moves in agreement with the change in the resonance condition. To find the plasma's lifetime, we measure the time it takes for the central density to drop to $\sim 70\%$ of its initial value. We do this both with the quadrupole field on and off, then compute the relative lifetime.

We model the results of our experiments by constructing a diffusion coefficient, $D = \lambda^2 \nu f$, where λ is the average step size of a resonant electron, ν is the fre-
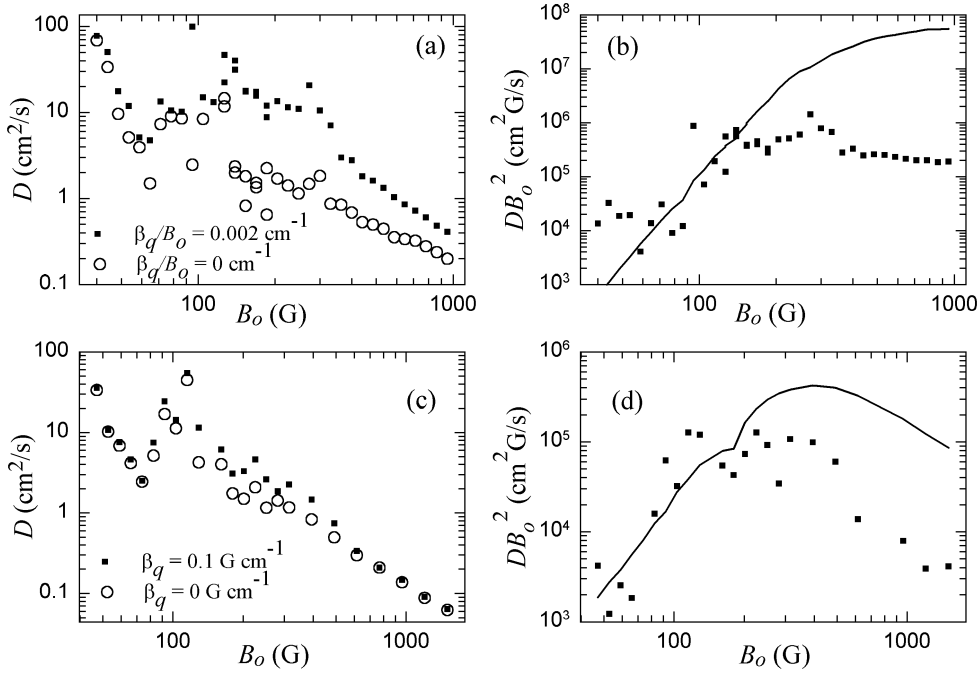
FIGURE 7. (a) D for $\beta_q/B_o = 0, 0.002 \text{ cm}^{-1}$. (b) D due only to the quadrupole field. Above $B_o \sim 200$ G, D scales roughly like B_o^2. (c) D for $\beta_q = 0, 0.1 \text{ G cm}^{-1}$. (d) Near resonance, D due to the quadrupole field is enhanced. In (b) and (d), the solid curve is $D(n, kT, B_o)$ from the theory using the measured densities at each point and assuming $kT = 1.5$ eV.

quency of collisions that knock an electron out of resonance, and f is the fraction of electrons that satisfy the resonance condition. We must sum over the higher order resonances to obtain an expression for D. The result is $D = \sum_{N \text{ Odd}} D_N$, where, for a constant density plasma,

$$D_N = \frac{2R^2 n^2 e^2}{\pi^4 \epsilon_o^2} \sqrt{\frac{m}{2\pi kT}} \left(\frac{\beta_q}{B_o}\right)^2 \frac{L^3}{N^5 B_o^2} \exp\left(\frac{-v_N^2}{v_{th}^2}\right). \tag{4}$$

This formula, suitably generalized for arbitrary $n(r)$, is used in Fig. 7 (b,d).

Clear evidence for resonant particle transport as the mechanism for plasma loss in Malmberg-Penning traps has been lacking. When applying a magnetic quadrupole perturbation, we observe resonant behavior that could help to explain plasma loss in Malmberg-Penning traps. If operating in suitable parameter regime, experiments planned by the ATHENA and ATRAP collaborations may be able to use both Malmberg-Penning traps and quadrupole traps. For example, if ATRAP operates with $B_o = 2$ T, $n = 10^8 \text{ cm}^{-3}$, $L = 1$ cm, and $T = 4$ K [6], they will be near the resonant axial field of 0.7 T and plasma loss due to the quadrupole field may be too great to tolerate.
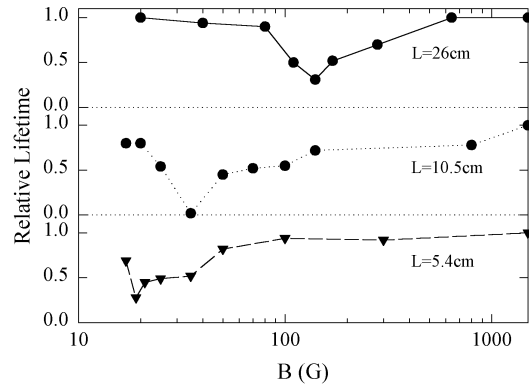
FIGURE 8. Graphs of the relative lifetime versus magnetic field show that when the resonance condition is met, particle loss is enhanced. The resonance location is length dependent.

ACKNOWLEDGMENTS

REFERENCES

1. D. L. Eggleston, T. M. O'Neil, and J. H. Malmberg, Phys. Rev. Lett. **53**, 982 (1984).
2. D. L. Eggleston and J. H. Malmberg, Phys. Rev. Lett. **59**, 1675 (1987).
3. D. L. Eggleston, Phys. Plasmas **4**, 1196 (1997).
4. D. L. Eggleston, Bull. Am. Phys. Soc. **43**, 1805 (1998).
5. J. M. Kriesel, Ph.D. thesis, University of California, San Diego, 1999.
6. G. Gabrielse, (private communication, 1999).